Sixth Japan-Canada Microscopy Societies Joint Symposium 2025

第6回　日本-カナダ顕微鏡学会交流シンポジウム 2025

Quantitative imaging and in-depth analysis in nanoscience

ナノサイエンスにおける定量イメージングと深層解析

June 9 - 10, 2025
Fukuoka International Congress Center
Fukuoka, Japan
(and Web Connection)

Japanese Society of Microscopy (JSM)
Microscopy Society of Canada (MSC)

This symposium is held with the 81st Annual Meeting of the Japanese Society of Microscopy.

The publication of this abstract book is supported by JSPS KAKENHI,
Grant Number [JP H25H00808].

Sixth Japan-Canada Microscopy Societies Joint Symposium 2025

	Time (Tokyo)	Speakers	Time (Winnipeg)
Session 1	**June 9, Monday**	**Fukuoka International Congress Center, Hall-G**	**June 8, Sunday**
	8:30 ～ 8:50	Connecting	6:30 pm ～ 6 :50 pm
	8:50 ～ 9:00	**Opening address**: President of JSM	6:50 pm ～ 7:00 pm
	9:00 ～ 9:30	**C-1**: Maureen J. Lagos (McMaster University)	7:00 pm ～ 7:30 pm
	9:30 ～ 10:00	**C-2**: Jane Y. Howe (University of Toronto)	7:30 pm ～ 8:00 pm
	10:00 ～ 10:30	**J-1**: Katsuaki Nakazawa (NIMS)	8:00 pm ～ 8:30 pm
	10:30 ～ 11:00	**C-3**: Shumeng Jia (McGill University)	8:30 pm ～ 9:00 pm
	11:00 ～ 11:30	**J-2**: Daiko Takamatsu (Hitachi, Ltd.)	9:00 pm ～ 9:30 pm
	11:30 ～ 12:00		
	12:00 ～ 12:50	Luncheon Seminar	
Session 2	**June 10, Tuesday**	**Fukuoka International Congress Center, Hall-G**	**June 9, Monday**
	8:40 ～ 9:00	Connecting	6:40 pm ～ 7:00 pm
	9:00 ～ 9:30	**J-3**: Kiyofumi Takaba (Univ. of Viena)	7:00 pm ～ 7:30 pm
	9:30 ～ 10:00	**C-4**: Marek Malac (NRC-Nano, Univ. of Alberta)	7:30 pm ～ 8:00 pm
	10:00 ～ 10:30	**J-4**: Takuma Toyonaga (Tohoku University)	8:00 pm ～ 8:30 pm
	10:30 ～ 11:00	**C-5**: Raynald Gauvin (McGill University)	8:30 pm ～ 9:00 pm
	11:00 ～ 11:30	**J-5**: Shigeo Mori (Osaka Metropolitan University)	9:00 pm ～ 9:30 pm
	11:30 ～ 11:40	**Closing address**: President of MSC	9:30 pm ～ 9:40 pm
	11:40 ～ 12:00		
	12:00 ～ 13:30	JSM Annual General Meeting	

Official site: https://www.omu.ac.jp/eng/japan-canada-microscopy-seminar/
Contact: gr-eng-JapanCanadaSeminar@omu.ac.jp

URL of web-site connection for hybrid meeting

Session 1 June 9, 2025 8:50 – 11:30 am Tokyo time

Fukuoka International Congress Center, Fukuoka, Fukuoka, Japan
https://us06web.zoom.us/j/82499795626?pwd=NcREJDGEjrOKoa29cybwm179rLT64k.1
Webinar ID: 824 9979 5626
Passcode: 380579

Session 2 June 10, 2025 09:00 – 11:40 am Tokyo time

Fukuoka International Congress Center, Fukuoka, Fukuoka, Japan
https://us06web.zoom.us/j/86910676923?pwd=NabT6brEQ5ygMf1OH0ymqCrQV0pPaa.1
Webinar ID: 869 1067 6923
Passcode: 717117

【Preface】

Dear Participants,

It is our great pleasure to welcome you to the 6th Japan–Canada Microscopy Societies Joint Symposium.

Since its launch in 2020, this symposium has served as an important platform for scientific collaboration between the Japanese Society of Microscopy (JSM) and the Microscopy Society of Canada (MSC), bridging communities across materials and life sciences. This year, we are pleased to hold the event in a hybrid format, with both in-person sessions in conjunction with the JSM annual meeting and online participation, allowing broader international engagement.

The theme of this year’s symposium, "Quantitative imaging and in-depth analysis in nanoscience," reflects the growing importance of precise measurement and deep analytical insight in understanding nanoscale systems. We hope this symposium will foster discussion, inspire new research directions, and deepen the collaboration between Japan and Canada in the field of microscopy.

As we gather for this year’s symposium, we would like to take a moment to express our heartfelt condolences on the passing of Dr. Misa Hayashida, who was instrumental in the establishment and ongoing success of this joint symposium series. Her dedication and spirit of cooperation have left an enduring legacy within our communities. Her contributions will continue to inspire us in the years to come.

This year’s program features outstanding contributions from early-career and renowned researchers, highlighting the dynamic research landscape in both countries. We believe the presentations and discussions will be of great benefit to all participants and will further strengthen academic and personal ties between our societies.

We would like to extend our sincere appreciation to all those who made this event possible, especially Professor Shigeo Okabe of President of JSM, and Professor Yasukazu Murakami of the chairperson of the 81st Meeting of JSM.

We hope this symposium will be a rewarding and memorable experience for all.

Sincerely yours,

Organizers
Kodai Niitsu (National Institute for Materials Science)
Shigeo Mori (Osaka Metropolitan University)
Ken Harada (Osaka Metropolitan University)
Marek Malac (NRC-NANO and University of Alberta)
Makoto T. Schreiber (NRC-NANO and University of Alberta)

【Greetings】

Dear Esteemed Colleagues,

On behalf of the Japanese Society of Microscopy, I am both delighted and honored to welcome you to the Sixth Japan-Canada Microscopy Societies Joint Symposium 2025. This event will be held at the Fukuoka International Congress Center on June 9th and 10th, 2025, in Hakata, Fukuoka, Japan.

This year’s symposium theme, “Quantitative Imaging and In-Depth Analysis in Nanoscience” will unite the latest advancements in imaging techniques and corresponding analytical methods in nanoscience from Canada and Japan. Indeed, the quantitative extraction of valuable information from images forms the foundation of solid microscopical work. Distinguished speakers from both countries will present their cutting-edge research results and technologies, generating significant interest among a diverse range of scientists and engineers. I sincerely hope that the symposium will provide an excellent opportunity for researchers to network, especially for young students.

I extend my heartfelt gratitude to the sponsoring organizations and the volunteer organizers in Japan and Canada. Last but not least, I would like to express my appreciation for Dr. Misa Hayashida, whose enthusiastic efforts have helped bridge the two societies over the years. Tragically, she passed away in July 2024, and we will miss her dearly. I sincerely hope the strong ties between Canada and Japan will continue to honor her memory.

I am eagerly looking forward to the symposium, featuring prominent scientists from both countries, where we will share new and exciting research in electron microscopy and related technologies.

Yours sincerely,

Hiroshi Jinnai, (Tohoku University)
President-Elect
The Japanese Society of Microscopy

【Greetings】

Dear Esteemed Colleagues,

It is my great pleasure to welcome you all to this joint workshop between the Microscopy Society of Canada (MSC) and the Japanese Society of Microscopy (JSM), held as part of annual conference of the JSM in Fukuoka, Japan, and MSC here in Winnipeg, Canada.

This event is a testament to the power of international collaboration in advancing the field of microscopy. We are truly honored to host such a distinguished group of speakers from both Japan and Canada—experts who are not only leaders in their respective areas, but also passionate about pushing the boundaries of imaging science. The quality of today's program reflects the depth and breadth of talent in both our communities.

We are fortunate to build upon a foundation of already fruitful collaborations between Canadian and Japanese researchers. These partnerships have led to impactful scientific discoveries and enduring professional relationships. One of the primary goals of today's workshop is to not only celebrate these successes, but also to inspire new connections and collaborations. Whether you're just starting out in your career or are a seasoned researcher, I encourage everyone to take advantage of the rich networking opportunities available throughout the conference.

Events like this don't happen without careful planning and dedication. I would like to extend my sincere thanks to Ken Harada (Osaka Metropolitan University, Japan), Kodai Niitsu (National Institute for Materials Sciences, Japan), Shigeo Mori (Osaka Metropolitan University, Japan), and in Canada Marek Malac (National Research Council, Canada), Makoto Schreiber (University of Alberta, Canada) whose efforts in organizing this workshop have been invaluable. Their commitment to fostering international scientific dialogue has made today possible. I would also like to acknowledge Misa Hayashida (National Research Council, Canada) who was key in establishing the joint JSM-MSC symposium and co-organizing it for the first five years.

I wish you a stimulating and productive discussions, and I hope this workshop will mark the beginning of many new collaborative ventures between our societies.

Thank you and enjoy the workshop!

Nadi Braidy, (Université de Sherbrooke)
President of Microscopy Society of Canada

【Scientific Program】

Session 1　(Tokyo time: Monday, June 9, 2025)

Web connecting　08:30 – 08:50

Opening address　08:50 – 09:00

Prof. Hiroshi Jinnai (President-Elect of JSM)

C-1　09:00 – 09:30

Maureen J. Lagos (McMaster University)

Launching hyperbolic phonon polaritons in twisted bilayers with electrons

C-2　09:30 – 10:00

Jane Y. Howe (University of Toronto)

Can We Perform Secondary Electron Imaging in Liquid-Phase SEM?
A Monte Carlo Simulation Study

J-1　10:00 – 10:30

Katsuaki Nakazawa (National Institute for Materials Science)

Development of 5D-STEM Method for Analyzing Amorphous Materials

C-3　10:30 – 11:00

Shumeng Jia (McGill University)

Advancing X-ray Micro-computed Tomography Image Processing of Avian Eggshells: An Improved Registration Metric for Multiscale 3D Images and Resolution-enhanced Segmentation using Edge-attentive Neural Networks

J-2　11:00 – 11:30

Daiko Takamatsu (Hitachi, Ltd.)

Visualization of the dynamic relocation of electrocatalysts during H_2O/CO_2 electrolysis using synchrotron X-ray microscopy

Session 2 (Tokyo time: Tuesday, June 10, 2025)

Web connecting 08:40 – 9:00

J-3 09:00 – 09:30

Kiyofumi Takaba (University of Vienna)

An electron diffractometer with the JUNGFRAU detector with large scale capacity

C-4 09:30 – 10:00

Marek Malac (NRC-Nano, University of Alberta)

NanoMi (ナノ美): Horizontal Column and Scanning Unit Development

J-4 10:00 – 10:30

Takuma Toyonaga (Tohoku University)

Cryo-EM Analysis of Chained G_1-ATPase, Motor for *Mycoplasma* Gliding

C-5 10:30 – 11:00

Raynald Gauvin (McGill University)

State-of-the-art Analytical Characterization of Lithium with a low Voltage TEM

J-5 11:00 – 11:30

Shigeo Mori (Osaka Metropolitan University)

Deterioration Mechanisms due to Exposing to Humidity-Controlled Air in All Solid-State Battery Revealed by TEM

Closing address 11:30– 11:40

Prof. Nadi Braidy (President of MSC)

Session 1 C-1

Launching hyperbolic phonon polaritons in twisted bilayers with electrons

Ka Yin Lee[1], Yina Wu[2], Javier Garcia de Abajo[2], and Maureen J. Lagos[1]*

[1] Department of Materials Science and Engineering, McMaster University, Hamilton, Canada
[2] The institute of Photonic Sciences (ICFO), Barcelona, Spain
*mjlagos@mcmaster.ca

We will discuss the physics of the excitation of hyperbolic polaritons sustained in twisted low symmetry bilayers (e.g. β-Ga_2O_3, α-MoO_3) using an atom wide electron beam with sub-5 meV energy resolution [1]. The focus will be on discussing the launching and spectroscopy of hyperbolic phonon modes. We fabricated suspended single and twisted bilayer structures. We demonstrated that thin β-Ga_2O_3/α-MoO_3 slabs can support a large variety of hyperbolic polaritons over a broad region of the mid-infrared range, with highly directional propagation directions. Twisting effects play a role in the formation of skew scattering patterns near surfaces, as well as in the polariton spatial distribution. Simulations of the inelastic electron scattering revealed the role of thickness in the twisting effects and the dynamics of launched polaritons. Depending on the tuning angle the polariton propagation direction can be steered. These findings expand our understanding of propagation of hyperbolic phonon polaritons in twisted bilayers.

Reference :

[1] M. J. Lagos, et al., *Microscopy* **71** (2022) i174.

Can We Perform Secondary Electron Imaging in Liquid-Phase SEM? A Monte Carlo Simulation Study

Jane Howe[1]*, Dian (Jack) Yu[1], Mia San Gabriel[1], Keryn Lian[1], and Stas Dogel[2]

[1] Department of Materials Science and Engineering, University of Toronto, 184 College Street, Toronto, M5S 3E4, ON, Canada
[2] Hitachi High-Tech Canada, Inc., 89 Galaxy Boulevard, Etobicoke, M9W 6A4, ON, Canada
*jane.howe@utoronto.ca

Scanning electron microscopy (SEM) employs both secondary electrons (SE) and backscattered electrons (BSE) for imaging and visualization of samples. Secondary electrons, with a cut-off energy of 50 eV, are created when inelastic scattering of the beam electrons ejects low-energy electrons of the specimen. SE has the most characteristic feature of low kinetic energy. Therefore, although SE are generated along the complete trajectory of the beam path within the specimen, only a very small fraction of SE reach the surface with sufficient kinetic energy to exceed the surface energy barrier and escape [1]. In the liquid-phase SEM studies using electron-transparent Si_3N_4 membrane window, most of the studies use backscattered electrons (BSE) with a high incident electron energy of 10 keV or higher for imaging [2-4]. The conventional wisdom behind such practice is the higher kinetic energy of BSE would lead to better signal to noise (S/N) ratio and contrast in liquid-phase imaging.

We ask the question whether SE imaging is a viable means of visualization in the liquid-phase SEM environment. A Monte-Carlo simulation workflow, based on the open-source software package Nebula [5], was developed to significantly reduce computation time without compromising the accuracy of the results. We studied effects of thickness and composition of specimen, thickness of window membrane, and incident electron energy on the visibility of specimen in liquid-phase SEM based on Si_3N_4 membrane. Shown in Fig. 1, by using a thin wedge as the specimen geometry and non-uniform spacing of the scan points, we avoided the need to generate numerous geometries for each configuration and reduced the computation time by up to 2 orders of magnitude. We carried out quantitative analyses of the threshold current for visible contrast and the spatial resolution. It shows that SE may be more effective in imaging thin specimens than BSEs at incident electron energies down to 3 kV when aided by efficient in-lens detectors and thin Si3N4 window with a thickness of 20 nm or less. The simulations also supported the trends of decreasing spatial resolution with increasing thickness of both the membrane and the specimen. The experiments were conducted using a Hitachi SU7000 SEM with a liquid cell. Figure 2 presents both SE and BSE images of bentonite clay through 20 nm thick Si_3N_4 window from 2 to 20 kV. SE imaging at 3 kV gives the best combination of resolution and S/N ratio. Despite the limitations of the software, which takes no consideration of radiolysis, charging, contamination, optical aberrations, and external field effects, the simulated results still provided a quantitative guidance for designing experiments and data interpretation.

Acknowledgements: Research sponsored by the NSERC Discovery Grant and CRDPJ grant, and Canada Foundation for Innovation's IF and JELF grants.

References:

1. Goldstein JI et al, Scanning Electron Microscopy and X-Ray Microanalysis, fourth ed, Springer, New York NY, 2018.
2. Thiberge S et al, Review of Scientific Instruments (2004) **75**, 2280–2289.
3. Kolmakov A in Liquid Cell Electron Microscopy, Ross FM (Ed.) Cambridge, UK, Cambridge University Press; 2016, 78–105.
4. de Jonge N and Ross MF, Nature Nanotechnology (2011) **6**, 695–704.
5. van Kessel L and Hagen CW, SoftwareX (2020) **12**, 100605.

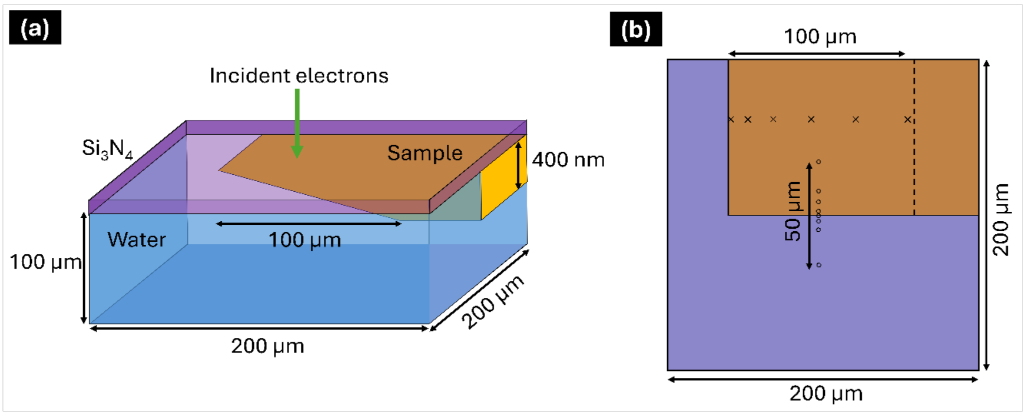

Fig. 1. Schematic of a wedge-shaped specimen through a SiN window in water. The sample geometry (a), and plan view of the specimen (b) with the non-uniform distribution of the scan points for contrast-thickness profile (horizontal array, crosses) and spatial resolution (vertical array, empty circles).

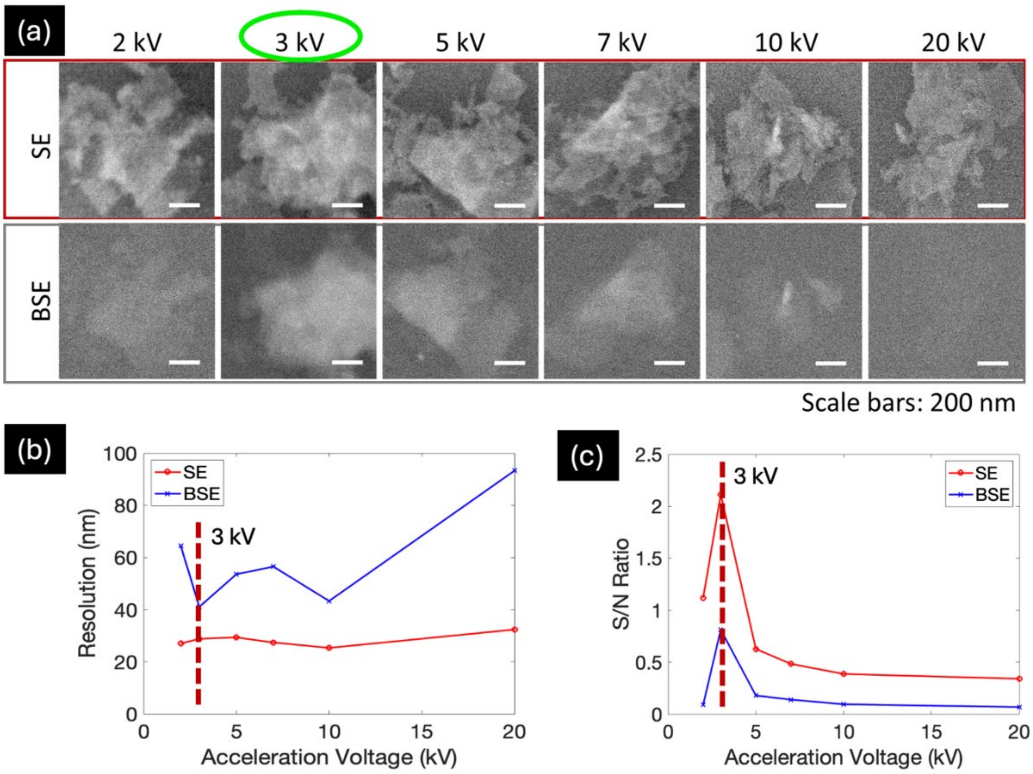

Fig. 2. Experimental data of liquid-phase SEM of bentonite clay through 20 nm thick SiN window in (a). Combined resolution (b) and S/N ratio (c) are the best at 3 kV from SE signals.

Development of 5D-STEM Method for Analyzing Amorphous Materials

Katsuaki Nakazawa（中澤 克昭）[1*]

[1] National Institute for Materials Science, 1-2-1, Sengen, Tsukuba, 305-0047, Japan.
*NAKAZAWA.Katsuaki@nims.go.jp

Unlike crystalline materials, amorphous materials lack a regular atomic structure, particularly in terms of long-range periodicity. As a result, each point within an amorphous material has a distinct atomic configuration. This structural heterogeneity leads to variability in physical properties, which also influences the macroscopic behavior of the material. Consequently, to effectively control and enhance the performance of amorphous materials, it is essential to pursue a three-pronged approach: measuring structural heterogeneity, observing the formation process of that heterogeneity, and evaluating the effects of heterogeneity on material properties.

In this study, we investigated the relationship between atomic-scale structural heterogeneity and the heterogeneity in dynamics of atomic motion. It is known that the atomic motion becomes heterogeneous near the glass transition temperature (T_g). This phenomenon is called dynamic heterogeneity and is believed to be the origin of the rapid increase of viscosity near T_g [1]. We employed convergent beam electron diffraction for the detection of the relationship between these heterogeneities. To visualize the atomic motion, the acquisition of the time distribution of diffraction patterns is required, and to elucidate its spatial heterogeneity, the acquisition of the spatial distribution of diffraction patterns is also required. Hence, it is required to record the spatiotemporal distribution of diffraction patterns. To achieve this requirement, I developed a five-dimensional scanning transmission electron microscopy (5D-STEM) method [2], which enabled us to record the spatiotemporal distribution of diffraction patterns. The 5D-STEM data enables us to analyze both heterogeneities, thereby clarifying the relationship between structural and dynamical heterogeneity. I estimated the local order of atomic structure via the variation of the intensity of the diffraction pattern, and the atomic motion via the temporal decay of the correlation of the time distribution of diffraction pattern. $Zr_{50}Cu_{40}Al_{10}$ was chosen as a sample whose T_g was 673K. I heat the sample from 633 K to 673K by using an in-situ heating holder. As a result, structural and dynamical heterogeneities are visualized simultaneously. As the temperature increased, the structural order decreased, and the atomic motion became faster. Finally, I measured the correlation between the heterogeneities and found a positive correlation between the heterogeneities, indicating that the ordered structures tend to have slow dynamics [3].

Furthermore, using this newly developed 5D-STEM, I examined the process by which crystals precipitate within a Fe-based metallic glass. Fe-based metallic glass is used as soft magnetic materials. To further enhance their functionality, there is a strong demand for materials with even lower coercivity. Because smaller grain sizes result in reduced coercivity, attention has been directed toward developing nanocrystalline soft magnetic materials. One example is FINEMET or NANOMET, which is produced by heat-treating Fe-based amorphous alloys to disperse α-Fe crystals (on the order of a few tens of nanometers in diameter) within the amorphous matrix. In the case of FINEMET, a small amount of Cu is added to promote nanocrystallization; three-dimensional atom probe studies have demonstrated that the added Cu forms clusters, which then act as nucleation sites for α-Fe crystallization [1]. Nevertheless, the nature of the atomic motions that occur near the crystallization temperature remains unclear. Therefore, in this study, we employed 5D-STEM to observe the crystallization process.

Acknowledgment:

This research was supported by JST-KAKENHI grant and ARIM of the MEXT. I thank the supports from Dr. K. Mitsuishi, Dr. S. Kohara, Dr. K. Tsuchiya, Dr. K. Niitsu, Prof. T. Ichitsubo, Prof. H. Kato, and Dr. T. Yamazaki.

References:

[1] L. Berthier and G. Biroli, Rev. Mod. Phys. **83**, 587–645 (2011).

[2] K. Nakazawa and K. Mitsuishi, Microscopy **72**, 446 (2023).

[3] K. Nakazawa et al., NPG. Asia. Mater. **16**, **57** (2024).

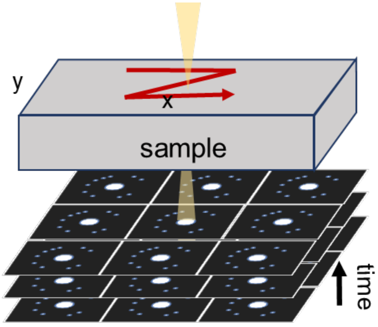

Fig. 1. Schematic of 5D-STEM. 5D-STEM obtains time resolution by repeating the 4D-STEM measurement.

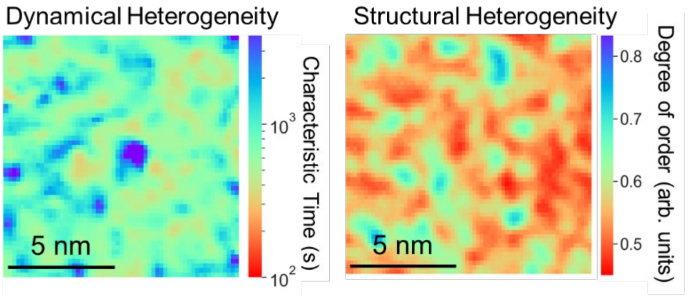

Fig. 2. Dynamical and Structural heterogeneities measured by 5D-STEM. The sample was heated at 633 K.

Session 1 C-3

Advancing X-ray micro-computed tomography image processing of avian eggshells: An improved registration metric for multiscale 3D images and resolution-enhanced segmentation using edge-attentive neural networks

Shumeng Jia[1], Marc D. McKe[2,3], and Natalie Reznikov[1,2,3*]

[1] Department of Bioengineering, McGill University, Montreal, Quebec, Canada
[2] Faculty of Dental Medicine and Oral Health Sciences, McGill University, Montreal, Quebec, Canada
[3] Department of Anatomy and Cell Biology, McGill University, Montreal, Quebec, Canada
*natalie.reznikov@mcgill.ca

Avian eggs exhibit a wide range of shapes and sizes, adapted to different reproductive strategies. Beyond providing physical protection, the shell is also a porous structure that helps regulate gas and water vapor exchange, which is essential for embryonic development. Among different species, pore morphology varies in size, shape, connectivity, and frequency, which is believed to be an adaptation to the environment in which they are incubated.

To date, numerous studies on eggshell regional ultrastructure have been performed on many avian species. However, our knowledge regarding the pore distribution across an entire eggshell is still limited. This limitation arises from an intrinsic trade-off in imaging: increased magnification often comes at the expense of context-providing field-of-view. Combining large volume and fine detail remains a significant challenge, and clearly identifying all pores on an eggshell in a nondestructive manner is impossible with existing scientific imaging techniques.

To overcome the resolution barrier and to simplify post-scanning image processing, a deep learning-based Generative Adversarial Network (GAN) was constructed to perform resolution enhancement of large-volume, low-resolution 3D tomographic data while simultaneously performing voxel-wise labeling. The output of this model is a fully analyzable segmentation in which the pores, shell, and background are accurately classified. The model was trained on 3D X-ray micro-computed tomography (X-ray microscopy) images of avian eggshells obtained from the Redpath Museum of McGill University, Montreal, Canada. Each egg was imaged with stepwise magnification to form superimposable low- and high-resolution training sets. Accurate registration of these multi-scale scans is crucial to ensure reliable model training and meaningful comparisons across different scales of features. Registration performance was validated using a novel evaluation metric which focuses on local grayscale gradients (edges) to quantify registration error and define alignment quality numerically rather than relying on human inspection. An edge-attentive loss function was also deployed to supervise model performance and balance the disparity between large and small regions, preventing the model's attention from being biased toward dominant but uninformative classes (Background: 95%) while neglecting minor but important ones (Eggshell: 5%; Pores: 0.1%).

Beyond eggshells, this work not only supports the scientific study of porous materials and other structures and objects, but it also expands opportunities for research in the life sciences in case where there exists hierarchical complexity, such as in bone, plants, and seashells. This approach offers great potential for improving the quality, understanding, and processing efficiency of 3D X-ray microscopy.

References:

[1] Riley et al., British poultry science, Vol.**55**, (2014), 311-320.
[2] Ahmad et al. Scientific Reports, Vol.**12**, (2022), 9533.

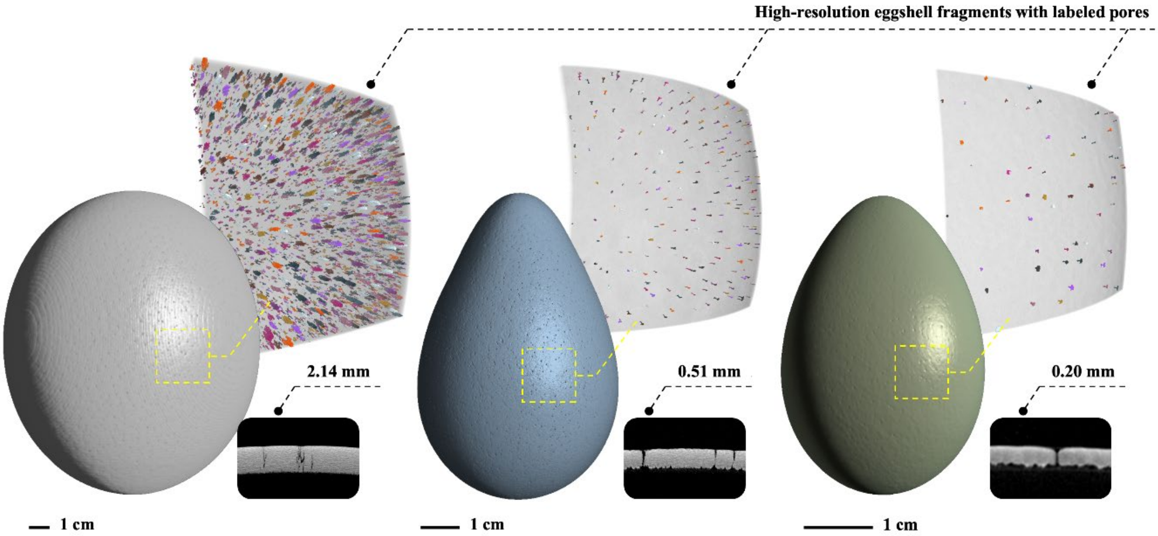

Fig. 1. Digital replicas of three museum eggshells: Ostrich (Struthio camelus), Thick-billed Guillemot (Uria lomvia), and American Crow (Corvus brachyrhynchos), from left to right (not to relative scale, but with scale bars indicated). A selected high-resolution eggshell volume from the equatorial region of the shell with pores identified using random distinct colors is displayed in the top-right field of each egg to illustrate variations in pore distribution among species. To the bottom-right of each egg, focusing on pore structures, is a single 2D cross-section taken from the X-ray microscopy imaging volume (shell thickness is annotated).

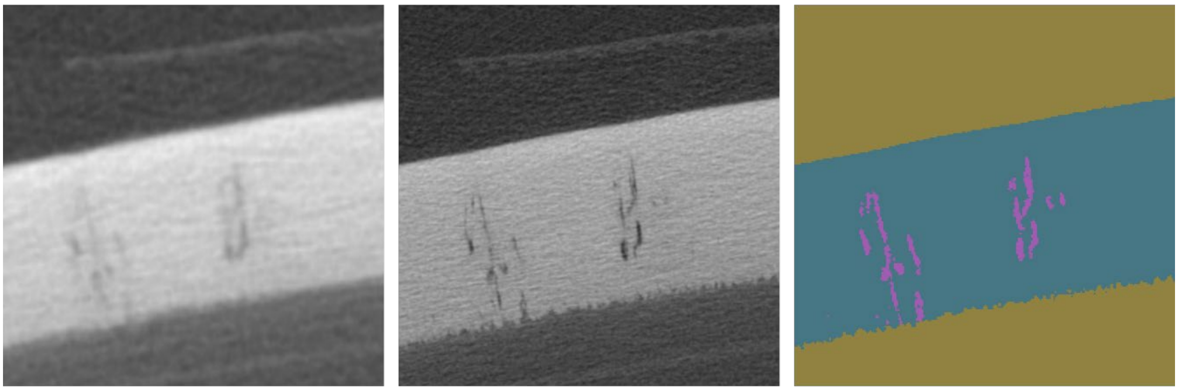

Fig. 2. From left to right: Ostrich eggshell scanned at low resolution (36 μm) as the learning input of the neural network, registered high-resolution (18 μm) image as the intermediate input, and high-resolution (18 μm) segmentation as learned by the model.

Session 1 J-2

Visualization of the dynamic relocation of electrocatalysts during H_2O/CO_2 electrolysis using synchrotron X-ray microscopy

Daiko Takamatsu（高松大郊）[1*], Akio Yoneyama[1], Tatsumi Hirano[1],
Naoto Fukatani[1], Kakuro Hirai[1], and Shin Yabuuchi[1]

[1] Research & Development Group, Hitachi, Ltd., 2520, Akanuma, Hatoyama-machi, Hiki-gun, Saitama, 350-0395, Japan
*daiko.takamatsu.hu@hitachi.com

Electrochemical devices such as batteries and electrolysis are composed of hierarchical structures in time and space, and the reaction processes in which these hierarchical structures are intricately related have a significant impact on cell performance. Therefore, to improve performance, it is necessary to fully understand the phenomena occurring inside the electrochemical cell during operation. We have developed *in situ* / *operando* and multiscale analysis techniques using synchrotron X-ray with appropriate temporal and spatial resolution to elucidate the reaction inhomogeneity and non-equilibrium / dynamic phenomena occurring inside the electrochemical cells such as lithium-ion batteries[1-3], lead-acid batteries[4], and thermo-electrochemical cells[5]. Recently, we have focused on the electrochemical devices that are attracting attention as a strategy to achieve carbon neutrality, namely H_2O electrolysis (green hydrogen production technology using renewable energy) and CO_2 electrolysis (technology that electrochemically reduces CO_2 and converts it into valuable chemicals). In this presentation, we will talk about the latest results of *ex situ* and *in situ* analysis of electrocatalysts in H_2O and CO_2 electrolysis using scanning X-ray fluorescence microscopy (SXFM).

Figure 1 shows the SXFM system conducted at the BL16XU of the SPring-8[6]. The monochromatized X-ray beam, generated by an undulate and Si (111) double-crystal monochromator (DCM), was focused onto a pinhole (virtual X-ray source) by a bend-cylindrical total reflection mirror. A focused micro-X-ray beam was formed by two elliptical total-reflection mirrors of Kirkpatrick-Baez configuration (KB mirrors) with a beam size of 1 μm square or less at the focal position. The X-ray microbeam was irradiated on the electrochemical cell capable to observe cross-sectional region placed on the xyz piezo stage, and the X-ray fluorescence generated from the cell was detected by the Silicon Drift Detector (SDD), which was positioned diagonally upstream of the cell.

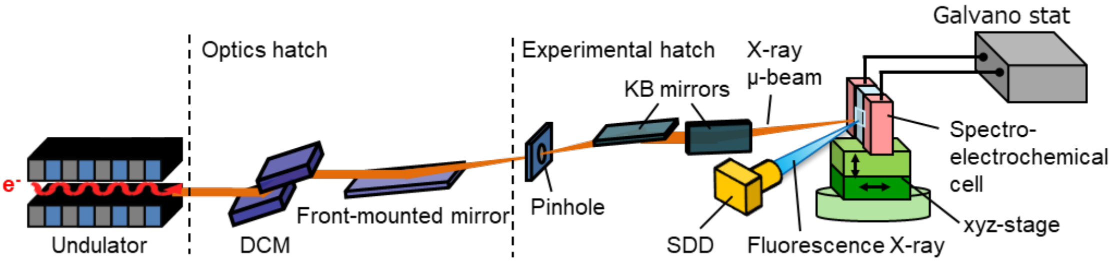

Fig. 1. Schematic diagram of the SXFM measurement system at SPring-8 BL16XU for *in situ* visualization of the behavior of electrocatalysts during operation.

The spectro-electrochemical cell for electrochemical CO_2 reduction reaction (CO_2RR) is composed of a Cu-catalyst gas diffusion electrode (Cu-GDE) cathode, a Pt anode, and a polymer electrolyte membrane (PEM), and gases and electrolytes can be introduced through current collectors with flow channels. Figure 2(a) shows the schematic of cross-sectional cathode region measured by *in situ* SXFM. Figure 2(b) shows the extracted Cu intensity maps of the cathode cross-sectional region during CO_2RR operation. Before the reaction, Cu catalyst layer was deposited on the GDE surface with a uniform thickness. However, during the reaction, Cu was observed not only near the GDE surface but also inside the GDE. After the reaction, Cu was dispersed inside the GDE. This indicates that Cu has migrated and relocated into the GDE during CO_2RR (Fig. 2(a)).

In the presentation, we will also show the results of *in situ* SXFM of the electrocatalyst during H_2O electrolysis and discuss the effect of the dynamic relocation of electrocatalyst on the performance of H_2O/CO_2 electrolysis.

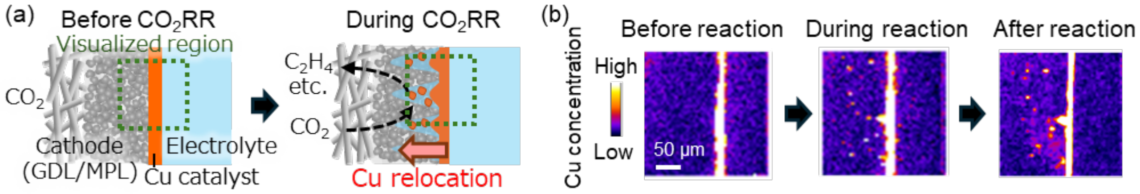

Fig. 2. (a) Schematic diagram of the cathode cross-sectional area visualized by *in situ* SXFM during CO_2 electrolysis. (b) Cu maps of the Cu-GDE obtained before, during and after CO_2RR.

References:

[1] D. Takamatsu et al., Angew. Chem. Int. Ed., **51**, 11597 (2012).

[2] D. Takamatsu et al., J. Phys. Chem. C, **119**, 9791 (2015)

[3] D. Takamatsu et al., J. Am. Chem. Soc., **140**, 1608 (2018).

[4] D. Takamatsu et al., Chem. Commun., **56**, 9553 (2020).

[5] D. Takamatsu et al., J. Mater. Res., **37**, 1576 (2022).

[6] A. Yoneyama et al., SUNBEAM Annual Report with Research Results, vol **1**, part 2, 38 (2011).

Session 2 J-3

An electron diffractometer with the JUNGFRAU detector with large scale capacity

Kiyofumi Takaba（高場圭章）[1*], Khalil Ferjaoui[2], Erik Fröjdh[2], Tim Gruene[1]

[1] Department of Inorganic Chemistry, University of Vienna, Währinger Straße 42, 1090 Vienna, Austria

[2] Photon Science Detector Group, Paul Scherrer Institute, 5232 Villigen, Switzerland

*kiyofumi.takaba@univie.ac.at

Since the 2010s, 3D electron diffraction (3D ED) has been used to reveal the atomic structure of small crystals (≤ 1 μm), which conventional X-ray diffraction cannot effectively analyze [1]. To meet the increasing demand for 3D ED in chemistry, mineralogy, and biology, it is crucial to advance the methodology in both hardware and software. The JUNGFRAU detector is a charge-integrating hybrid pixel detector, that has been originally developed for X-ray detection. This detector also offers significant advantages for the accurate detection of electrons [2].

We have developed a graphical user interface to operate 3D ED measurements using the JUNGFRAU 1M detector in conjunction with the JEOL JEM2100Plus electron microscope [3]. The frame stream, which runs at a rate of 2 kHz, can be saved with real-time summation via the Jungfraujoch FPGA-backend [4]. Data acquisition is synchronized with the control of the microscope using PyJEM, tagging the recorded HDF-formatted file with experimental parameters. Pipelined with processing software for crystallography, feedback is displayed instantaneously during the data collection session. These functions can determine the structure of a wide variety of molecules, and it is expected that the subatomic features, such as atomic charges [5], will become more generally available. Fig. 1 illustrates an overview of our workflow.

In this symposium, we will present our measurement workflow and the structures revealed. We will also discuss our future development directions and perspectives on diffraction imaging with electron microscopes and detectors.

References:

[1] T. Gruene *et al.*, *Angew. Chem. Int. Ed.* **57**, (2018), 16313-16317.

[2] E. Frojdh *et al.*, *Crystals* **10**, (2020), 1148.

[3] K. Ferjaoui *et al.*, “Graphical User Interface for JungFrau integrated in JEOL TEM”. https://github.com/epoc-ed/GUI (2024).

[4] F. Leonarski *et al.*, *J. Synchrotron Rad.* **30**, (2023), 227-234.

[5] K. Takaba *et al.*, *Nat. Chem.* **4**, (2023), 491-497.

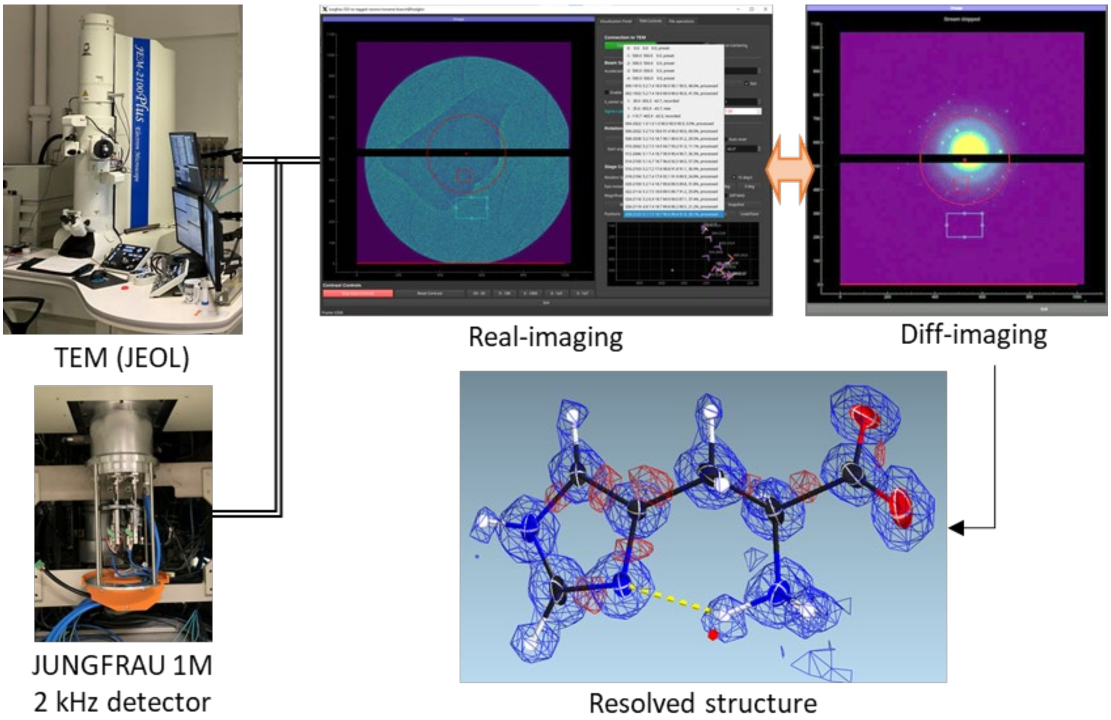

Fig. 1. Schematic workflow of 3D ED measurement using a dedicated GUI that integrates control of the JEOL TEM and the JUNGFRAU detector.

NanoMi (ナノ美): Horizontal Column and Scanning Unit Development

Marek Malac[1,2]*, Darren Homeniuk[1], Makoto Tokoro Schreiber[1,2], Mark Salomons[1], Sam Ruttiman[1,2], Xuanhao Wang[3], Ka Wing Kwan[1], Olivier Adkin-Kaya[4], Mohammad Kamal[4], Patrick Price[1], Martin Cloutier[1], Ray Egerton[2], Ken Harada[5]

[1]NRC-NANO, Edmonton, Alberta, Canada. [2]Dept. of Physics, U. of Alberta, Edmonton, Alberta, Canada. [3]Dept. Comp. Science, U of Alberta, Edmonton, Alberta, Canada. [4]Dept. El. and Comp. Eng, U. of Alberta, Edmonton, Canada. [5]RIKEN, Center for Emergent Matter Science, Hatoyama, Saitama 350-0395, Japan.

*mmalac@ualberta.ca

An open source (public license) electron microscopy platform, referred to as NanoMi (ナノ美), with modest target specifications, is being developed for educational purposes and for proof-of-principle experiments [1,2]. The instrument is designed for a maximum beam energy ≤50 keV, although ≤30 keV often appears to be sufficient, and results in lower cost than ≤50 keV option. To keep the manufacturing simple and cost-efficient, the column is based on electrostatic einzel lens, electrostatic deflectors and stigmators. The target resolution in TEM and STEM mode is 10 nm, but currently only about 200 nm has been demonstrated using a W-hairpin filament. TEM, SEM and electron diffraction capabilities have been demonstrated.

The use of electrostatic optics eliminates the need for water cooling and makes it easier to built and ultra-high vacuum-compatible instrument with its electron optics separated from the vacuum envelope. Fig. 1 shows one of the two NanoMi instruments in our laboratory, assembled on a ultrafast terahertz laser-optics bench. It routinely achieves $3\text{x}10^{-10}$ torr base pressure when pumped by 250 l/s turbomolecular pumps. The horizontal V-groove configuration makes optics reconfiguration convenient [2]. The vertical 5”-half pipe configuration is built using standard ConFlange$^{\text{TM}}$ hardware [2]. Current electron-optical elements are designed to fit a 2-inch outer diameter puck, but 50 mm outer diameter puck will be used for all future designs.

Recently, we have developed an FPGA-based scan reference signal generator and data collection system, Scan-O-Mi (Scan-O-美) [1]. It allows for images of up to 5,792 x 5,792 pixels collecting eight 16-bit depth channels simultaneously at 20 MHz. Since the X,Y outputs are 16 bit, the system allows for up to 64k x64k pixel image acquisition, as limited by on-board memory. Figure 2 shows an example of data acquired using Scan-O-Mi controlling beam of a Hitachi S-5500 ultra-high resolution SEM. The use of Scan-O-Mi demonstrates utility of NanoMi components for updates of commercial instruments. Python computer code as well as information on Scan-O-Mi can be downloaded from GitHub [1].

Acknowledgment:
Support for the project was provided by NRC-QN (NANO) and by NSERC RGPIN-2021-02539. M.M. wishes to acknowledge many years of insightful guidance provided by the late Dr. Misa Hayashida.

References:
[1] https://github.com/NanoMi-org and www.nanomi.org
[2] M. Malac et. al, *Micron* **163** (2022) 103362.

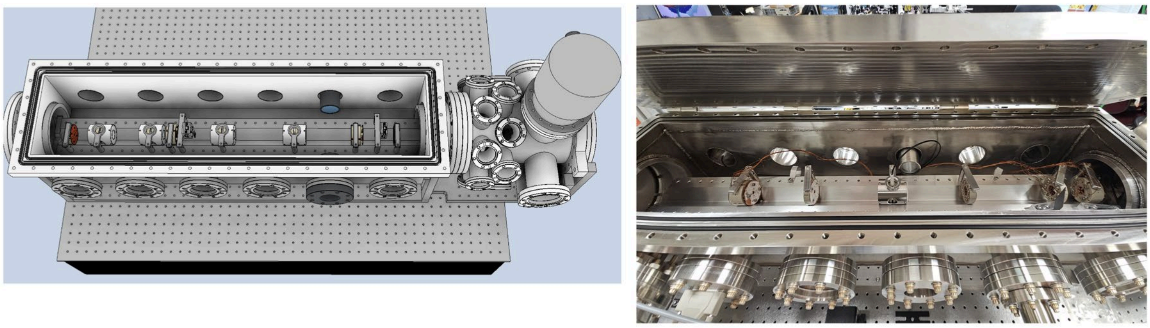

Figure 1. An example of NanoMi components utilized for development of a terahertz laser beam-controlled ultrafast electron microscope. The column is based on horizontal V-groove set up [2], electrostatic lens, and field-assisted (Schottky) thermal electron source. The entire NanoMi electron beam column is placed on an ultrafast laser-optics table.

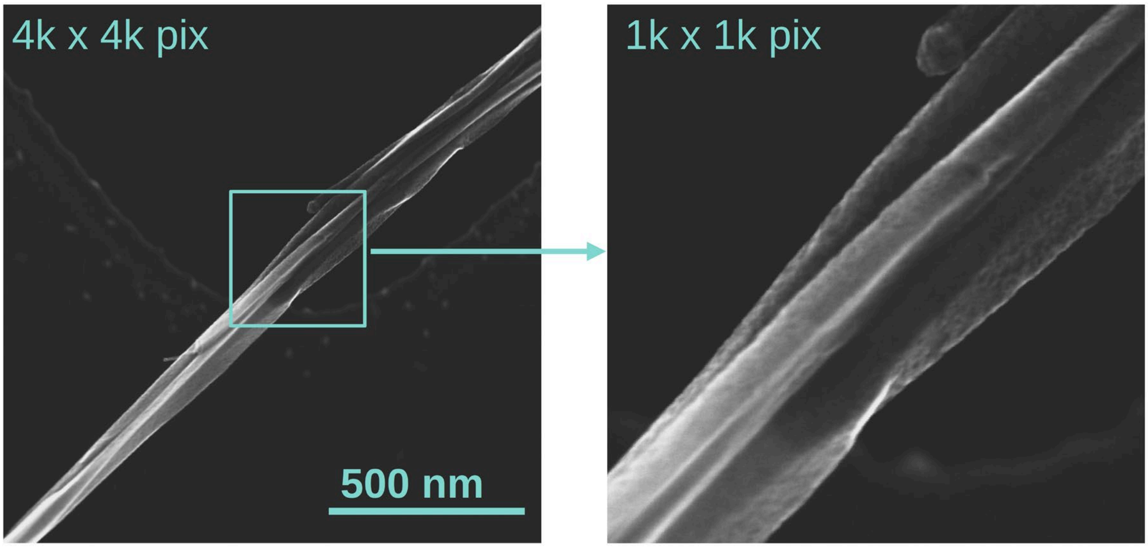

Figure 2. Scan-O-Mi scan reference signal generator and data collection unit was used to acquire images of ~90 nm diameter multi-wall carbon nanotubes on a Hitachi S-5500 ultra-high resolution scanning electron microscope. The Scan-O-Mi image on the left is 4k x4k pixels. The right image shows 1024 x 1024 pix area marked by a blue square in the full 4k x4k pix image.

Session 2 J-4

Cryo-EM Analysis of Chained G_1-ATPase, Motor for *Mycoplasma* Gliding

Takuma Toyonaga[1], Daisuke Unabara[1], Tasuku Hamaguchi[1],
Makoto Miyata[2], Koji Yonekura[1,3*]

[1] Institute of Multidisciplinary Research for Advanced Materials (IMRAM), Tohoku University, 2-1-1, Katahira, Sendai, Miyagi, 980-8577, Japan.
[2] Graduate School of Science, Osaka Metropolitan University, 3-3-138, Sugimoto, Osaka, Osaka, 558-8585, Japan.
[3] RIKEN SPring-8 Center, 1-1-1, Koto, Sayo, Hyogo, 679-5148, Japan.
*koji.yonekura.a5@tohoku.ac.jp

Rotary ATPases are molecular machines that couple rotational motion with ion transport across biological membranes [1]. ATP synthase, also known as F_1F_O-ATPase, is conserved across most organisms and functions both in ATP synthesis and membrane potential regulation. Interestingly, in the fish-pathogenic bacterium *Mycoplasma mobile*, the ATP synthase adopts an unprecedented chain-like complex that functions as a motor driving gliding motility (Fig. 1) [2]. We have designated this motor G_1-ATPase, identifying it as a novel member of the rotary ATPase family [3]. In the present study, to elucidate how this chain-like molecular motor powers *Mycoplasma* gliding motility, we performed single-particle analysis (SPA) of G_1-ATPase by cryo-EM using a CRYO ARM 300 II microscope. SPA is a technique that reconstructs three-dimensional protein structures from numerous particle images captured at various orientations.

Using a total of 59,504 particles, SPA of the G_1-ATPase unit in the presence of Mg^{2+} and ATP revealed three distinct structural states: state 1 (28,302 particles, 47.6%), state 2 (17,738 particles, 29.8%), and state 3 (13,464 particles, 22.6%) (Fig. 2). The dispositions of the central shaft (orange subunit) among these states suggest a rotational mechanism involving 120° steps, a feature conserved within the rotary ATPase family. Notably, only one of the two ATPases in the unit exhibited rotation of the central shaft, indicating that the two motors do not rotate synchronously. The relatively low particle count observed for state 3 implies that this state has a shorter lifetime during the 120° rotational cycle, suggesting catalytic coordination or interaction between the two ATPases. Furthermore, EM observations revealed how G_1-ATPase units are arranged in a chain-like formation. In this presentation, we propose a working model in which this chain-like rotary molecular motor drives the gliding motility of *Mycoplasma mobile*.

Acknowledgment:

This study was supported by a JST CREST grant (JPMJCR19S5) to M.M and Research Support Project for Life Science and Drug Discovery (Basis for Supporting Innovative Drug Discovery and Life Science Research (BINDS)) from AMED (JP23ama121006) to T.H. and K.Y.

References:

[1] AG. Stewart, M. Sobti RP. Harvey and D. Stock, Bioarchitecture, Vol. **3**, (2013), 2–12.

[2] M. Miyata and T. Hamaguchi, Current Opinion in Microbiology, Vol. **29**, (2016), 15-21.

[3] T. Toyonaga, T. Kato, A. Kawamoto, T. Miyata, K. Kawakami, J. Fujita, T. Hamaguchi, K. Namba and M. Miyata, Science Advances, Vol. **11**, (2025), eadr9319.

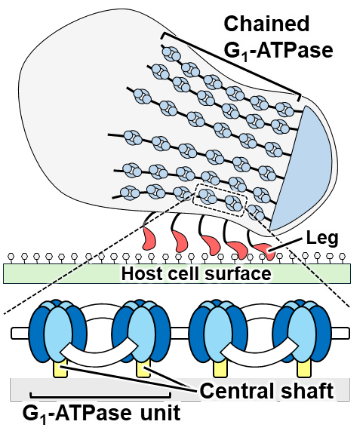

Fig. 1. Machinery for *Mycoplasma mobile* gliding motility. The chained G_1-ATPase associated with the cell membrane is depicted lower.

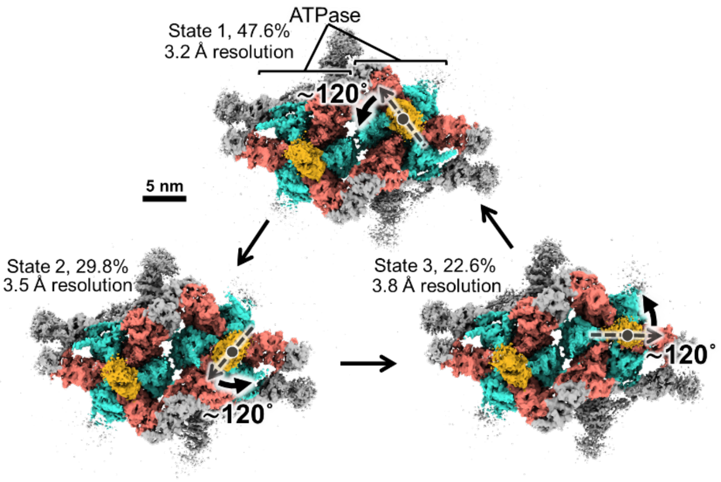

Fig. 2. Rotational mechanism of G_1-ATPase unit revealed by cryo-EM structures. Dotted arrows indicate the direction of central shaft.

State-of-the-art Analytical Characterization of Lithium with a low Voltage TEM

Raynald Gauvin, Stéphanie Bessette and Nicolas Brodusch

Department of Mining and Materials Engineering, McGill University,
Montréal, Québec, Canada, H3A 0C5.
*raynald.gauvin@mcgill.ca

This paper will present new achievements in performing quantitative EDS and EELS maps of lithium-based materials in the scanning electron microscope. State-of-the-art results acquired with the Hitachi SU-9000 dedicated STEM will be shown. This was the first SU-9000 to have EELS capabilities which allow Li detection [1]. It is also equipped with the Extreme EDS system from Oxford Instruments that can detect the K line of lithium [2]. The SU-9000 has a resolution of 0,22 nm in bright field STEM without aberration correctors and it allows lattice imaging.

Figure 1 shows a set of EDS maps acquired at 3 keV on Li_2CoSiO_4 for Co, Si, O, and Li as well as the corresponding sum spectrum. Clearly, the intensity of the Li map is much weaker than for the Co L, Si K, and O K lines. It is even possible to see that some 50 nm particulates are richer in Co. The sum spectrum shows that if there are Li K net X-ray intensities, it is very weak. The Li K map is likely to be the background map and possibly the Co M line that has an energy of 58 eV compared to 54,3 eV for Li K. The emission of the Li K line is difficult because of strong x-ray absorption in the material following ionization with a very weak fluorescence yield of roughly 1 over 10000. Also, the electrons coming from these two lines are from the valence band, and some of these electrons are likely to be bound to other elements, making the X-ray emission difficult, if not impossible. This was demonstrated in LiCl by Gauvin et al [3] where Li emission did not occur initially under electron irradiation but only after Cl evaporation following the formation of metallic Li where the electron could jump from the L to K shell. These results also showed that beam damage is common with the microanalysis of Li compounds.

Figure 2 shows an EELS spectrum of Spodumene, a Li_2FeSiO_4 mineral that accounts for about 40% of world Li production, taken with the Hitachi SU-9000 at 30 keV and with a cryo-holder at -155 °C. Even if X-ray emission was not detected with the EDS detector for this material for the same reasons stated above for Li_2CoSiO_4, the ionization edges are clearly visible for Fe, Li, and Si. This shows the strong advantage of EELS over EDS (or WDS) for Li quantification. This is clearly seen in figure [3] which shows a Li EELS edge to background ratio map of an Al-Li 2099 alloy recorded with the three-detectors system on the Hitachi SU-9000 at 30 keV. This map shows the round δ' precipitates (Al_3Li) of 5 to 20 nm and the T1 plates (AlCuLi) that have thicknesses between 1 to 2 nm. The fact that the edges are always ionized is a strong advantage for EELS. Also, the emission rate is greater than about 10,000 owing to the fluorescence yield. The downside of EELS is the need for a very thin transparent specimen and beam damage can also occur at 30 keV. Results obtained with a cryo-holder to evaluate possible minimization of beam damage will be presented.

References:

[1] N. Brodusch, H. Demers, A. Gellé, A. Moores and R. Gauvin (2019), Ultramicroscopy, **203**, pp.1-36.

[2] P. Hovington, V. Timoshevskii, S. Burgess, H. Demers, P. Statham, R. Gauvin, K. Zaghib (2016), Scanning, **38**, 6, pp. 571 – 578.

[3] R. Gauvin et al. (2021), Microscopy and Microanalysis, **27**, pp. 1868-1869.

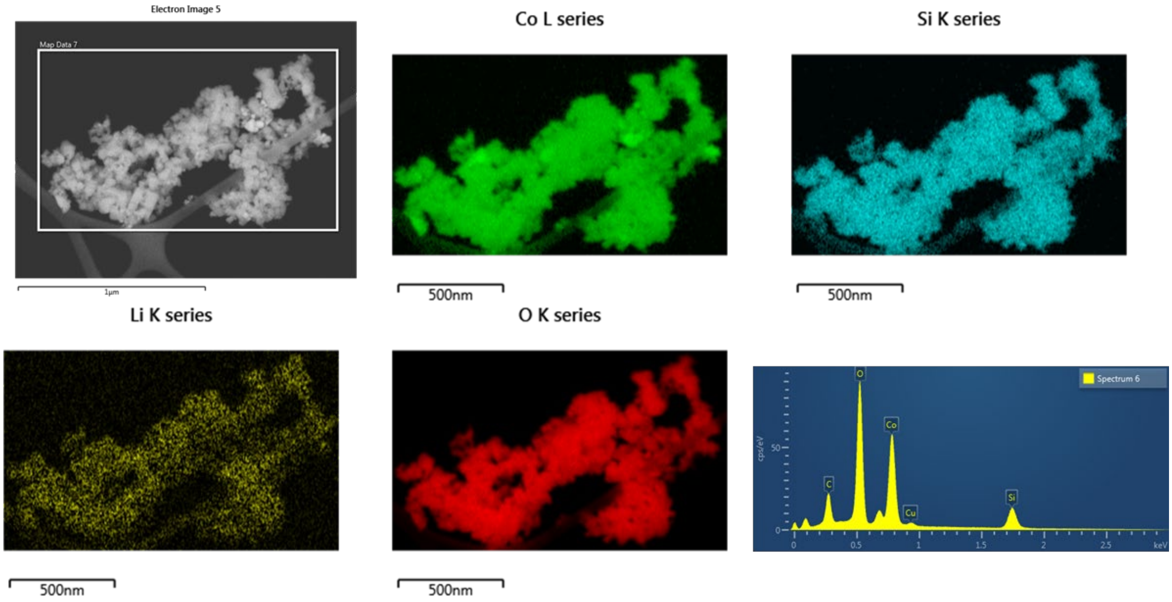

Figure 1. EDS map of Li_2CoSiO_4 acquired at 3 keV with the Extreme EDS detector installed on the Hitachi SU-9000. The Li map is a false map.

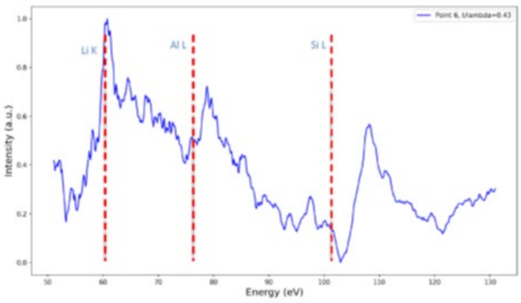

Figure 2. EELS spectrum of Spodumene, $LiAlSi_2O_6$, taken with the Hitachi SU-9000 at 30 keV and with a cryo-holder at -155 °C.

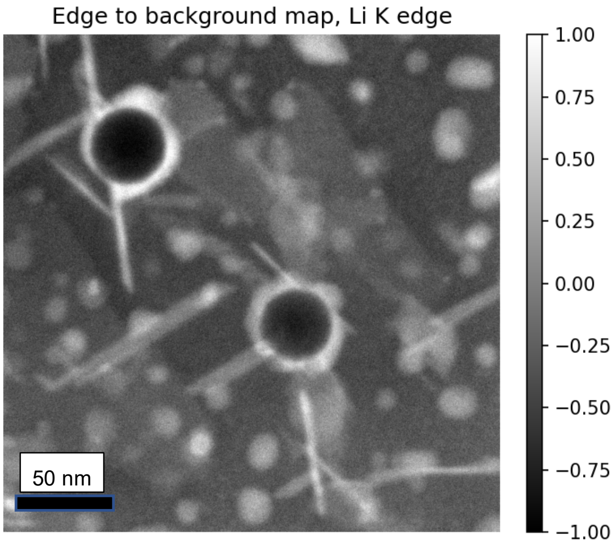

Figure 3. Li EELS edge to background ratio map of an Al 2099 alloy taken with the Hitachi SU-9000 at 30 keV.

Session 2 J-5

Deterioration Mechanisms due to exposing to Humidity-Controlled Air in All Solid-State Battery revealed by TEM

Shigeo Mori

Department of Material Science, Graduate School of Engineering, Osaka Metropolitan University, 1-1 Gakuen-cho, Naka-ku, Sakai, Osaka 599-8531, Japan

*moris@omu.ac.jp

All-solid-state lithium-ion batteries exhibit even higher energy densities owing to their flame retardancy and high thermal stability. Sulfide-based solid electrolytes (SEs) have recently attracted attention due to their high ionic conductivity comparable to that of an organic electrolytic solution [1]. However, their low moisture stability is a common disadvantage. Air exposure causes a significant decrease in their ionic conductivity, together with a toxic H_2S gas generation. This is a major barrier to all-solid-state cells fabrication process cost and its application to electric vehicles. Clarifying their deterioration mechanism during air exposure is necessary to develop sulfide-based SEs with high moisture durability.

As a promising SE for sulfide-based all-solid-state batteries, we focused on the argyrodite. Argyrodite-type crystals Li_6PS_5X (X = Cl, Br or I) have high ionic conductivities of 10^{-2}–10^{-3} S cm^{-1} at room temperature [2, 3]. In particular, Li_6PS_5Cl is reported to have a wide electrochemical window of up to 7.0 V vs. Li/Li$^+$ [3]. Furthermore, the all-solid-state cells using Li_6PS_5Cl and positive electrode materials such as Li_2S and $LiNi_{1/3}Co_{1/3}Mn_{1/3}O_2$ exhibit high electrochemical performance [4, 5]. Thus, Li_6PS_5Cl is a promising candidate SE for all-solid-state sulfide-based batteries. However, the moisture stability and structural changes it undergoes when exposed to humidified air are still unknown.

Recently we developed a transmission electron microscope (TEM) system to evaluate the air stability of battery materials. Using a vacuum transfer double-tilt TEM holder with a gas-flow system, the in situ observation of the degradation process was conducted for a sulfide-based Li_4SnS_4 glass ceramic under an air-flow environment. In this study, we conducted transmission electron microscope (TEM) observations in investigating the microstructure and morphology of argyrodite $Li_{7-a}PS_{6-a}Cl_a$ ($a \approx 1$, D_{50} = 3.5 μm, Mitsui Mining & Smelting, Japan) to understand its deterioration mechanism during air exposure. Figure 1(a) shows the electron diffraction pattern and its intensity profile after exposure to moisture at −20°C d.p. for 24 h. Diffraction peaks of Li_2CO_3 and LiCl are detected. These reaction products indicate that $Li_{7-a}PS_{6-a}Cla$ reacts with CO_2 and H_2O in the air [6]. In addition. We took the corresponding hollow-cone dark-field (HCDF) images and investigated the spatial distribution of the reaction products. Figures 1(b) and (c) show HCDF images obtained using the Debye-Scherrer rings of Li_2CO_3 and LiCl, respectively. Debye-Scherrer rings, which were used to capture the HCDF images, are indicated by the yellow highlighted areas in the ED patterns. Crystallite size is approximately 20–50 nm, as denoted by the bright contrast. Each reaction product is randomly distributed and deterioration seems to progress from the particle surface. In the presentation, the main factor of the decreased ionic conductivity and the deterioration process were discussed based on the reaction products caused by air exposure.

References:

[1] Y. Kato et al., Nat. Energy **1** (2016), 16030. doi: 10.1038/nenergy.2016.30

[2] M. A. Kraft et al., J. Am. Chem. Soc. **139** (31) (2017), 10909–10918. doi: 10.1021/jacs.7b06327

[3] S. Boulineau et al., Solid State Ionics **221** (2012), 1–5. doi: 10.1016/j.ssi.2012.06.008

[4] F. Han et al., Nano Lett. **16** (2016), 4521−4527. doi: 10.1021/acs.nanolett.6b01754

[5] J. Zhang et al., J. Power Sources **391** (2018), 73−79. doi: 10.1016/j.jpowsour.2018.04.069

[6] H. Tsukasaki et al., J. Power Sources **524** (2022), 231085. doi: 10.1016/j.jpowsour.2022.231085

Acknowledgement:

The authors thank all of the collaborators; Profs. H. Tsukasaki, A. Hayashi, A. Sakuta (Osaka Metropolitan University), Drs. H. Sano, Y. Morino (LIBTEC), Drs. K. Igarashi, A. Wakui, T. Yaguchi (Hitachi High-Tech Corporation). This study is based on results obtained from the project of "Development of Fundamental Technologies for All Solid State Battery applied to Electric Vehicles" (SOLiD-EV, JPNP18003) commissioned by the New Energy and Industrial Technology Development Organization (NEDO).

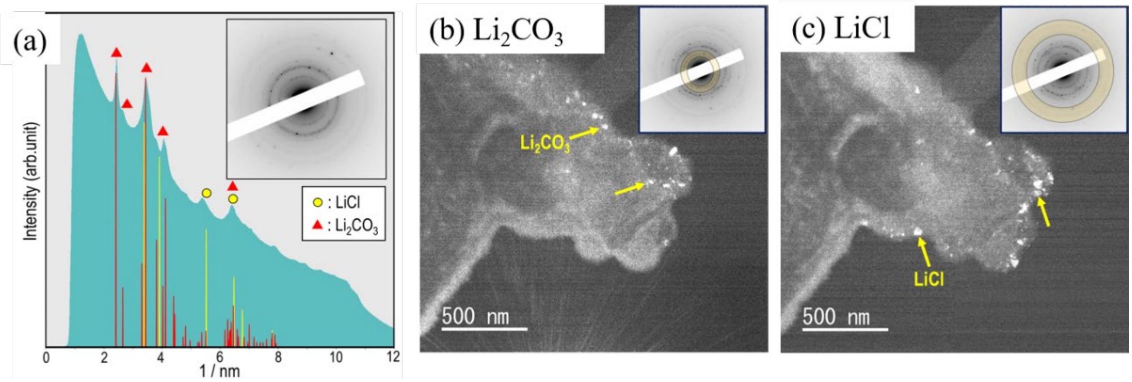

Figure 1. (a) Electron diffraction pattern and its intensity profile for $Li_{7-a}PS_{6-a}Cl_a$ after exposure to moisture of −20°C d.p. for 24 h. The HCDF images visualizing the size and spatial distribution of Li_2CO_3, and LiCl nanocrystallites. The images (b) and (c) were taken using the Debye-Scherrer rings of Li_2CO_3 and LiCl, respectively.

【Societies】

Japanese Society of Microscopy (JSM)
https://microscopy.or.jp/

Microscopy Society of Canada (MSC)
https://msc-smc.org/

【Venues】

Fukuoka International Congress Center （福岡国際会議場）
Hakata-ku, Fukuoka City, Fukuoka 821-0032, Japan
https://www.marinemesse.or.jp/congress/
https://www.marinemesse.or.jp/eng/

【Organizers】

Ken Harada (Osaka Metropolitan University)（原田研，大阪公立大学）
Kodai Niitsu (National Institute for Materials Science)
（新津甲大，物質・材料研究機構）
Shigeo Mori (Osaka Metropolitan University)（森茂生，大阪公立大学）
Marek Malak (NRC-NANO, University of Alberta)
Makoto T. Schreiber (NRC-NANO, University of Alberta)

【Technical Assistants】

Haruka Sanada (Osaka Metropolitan University)（眞田春佳，大阪公立大学）

【Contact】

Official site:
https://www.omu.ac.jp/eng/japan-canada-microscopy-seminar/english/index.html
Office e-mail: gr-eng-JapanCanadaSeminar@omu.ac.jp

【Misa Hayashida student scholarship】（林田美咲記念 研究奨励金 制度）

The scholarship has been established in memory of Dr. Misa Hayashida, a talented researcher who made important contributions to development and applications of electron microscopy. Misa’s contributions to science were stopped by her passing at an early age. The scholarship aims to preserve her curious spirit and her love for scientific discovery.

Thanks to generous support of Misa's family and friends, the scholarship is welcomes young microscopy researchers from both Canada and Japan with the aim of fostering relations between the Microscopy Society of Canada (MSC) and the Japanese Society of Microscopy (JSM).

https://msc-smc.org/award/misaschol.aspx
https://microscopy.or.jp/jp-ca_symposium/2025/hayashida.html